NASA Technical Memorandum 87004

Vibration and Buckling of Rotating, Pretwisted, Preconed Beams Including Coriolis Effects

K.B. Subrahmanyam and K.R.V. Kaza
Lewis Research Center
Cleveland, Ohio

Prepared for the
10th Biennial Design Engineering Conference and Exhibit
on Mechanical Vibration and Noise
sponsored by the American Society of Mechanical Engineers
Cincinnati, Ohio, September 10–13, 1985

NASA

VIBRATION AND BUCKLING OF ROTATING, PRETWISTED, PRECONED BEAMS INCLUDING CORIOLIS EFFECTS

K.B. Subrahmanyam[1] and K.R.V. Kaza
National Aeronautics and Space Administration
Lewis Research Center
Cleveland, Ohio 44135

ABSTRACT

The effects of pretwist, precone, setting angle and Coriolis forces on the vibration and buckling behavior of rotating, torsionally rigid, cantilevered beams are studied in this investigation. The beam is considered to be clamped on the axis of rotation in one case, and off the axis of rotation in the other. Two methods are employed for the solution of the vibration problem: one based upon a finite-difference approach using second order central differences for solution of the equations of motion, and the other based upon the minimum of the total potential energy functional with a Ritz type of solution procedure making use of complex forms of shape functions for the dependent variables. Numerical results obtained by using these methods are compared to those existing in the literature for specialized simple cases. Results indicating the individual and collective effects of pretwist, precone, setting angle, thickness ratio and Coriolis forces on the natural frequencies and the buckling boundaries are presented and discussed. Furthermore, it is shown that the inclusion of Coriolis effects is necessary for blades of moderate to large thickness ratios while these effects are not so important for small thickness ratio blades. Finally, the results show the possibility of buckling due to centrifugal softening terms for large values of precone and rotation.

INTRODUCTION

An important phase in the development of advanced turboprop blades currently in progress at the Lewis Research Center is the development of analytical blade models that are capable of predicting the vibration and flutter characteristics to an acceptable degree of accuracy. The turboprop blades are of thin cross sections with large, variable sweep and pretwist, and are mounted on a rotating hub at a setting angle. Moreover, the blades are subjected to considerable centrifugal loading and develop steady-state deflections that are large compared to the cross-sectional dimensions. These blades, under certain conditions are subjected to centrifugal compressive forces on certain cross sections, and consequently the possibility of buckling cannot be ruled out. The recent research in the vibration and flutter of these blades indicate that the effects of nonlinearities, variable sweep, and pretwist must be included in the analysis for accurate prediction of the blade dynamic characteristics. The finite-element modelling of these blades is appropriate for the determination of their dynamic characteristics. However, such studies with the existing codes showed that the predicted results are satisfactory only for the first few modes and that the complicating effects included in these theories make the understanding of the individual and collective effects of the governing parameters impossible. These considerations have lead to the modelling of the turboprop blade configurations using the simpler beam theories with the complicating effects successively taken into account to establish a physical understanding and to reveal the relative importance of the individual effects. A preliminary part of such study using a simplified beam model with a set of linear equations of motion is reported in this paper. In the beam model the effects of sweep on the dynamic behavior of the blade are introduced by setting the axis of the blade at an angle with respect to the plane of rotation. This angle is usually called the precone angle. The more complicated nonlinear aspects form the subject matter of a subsequent paper.

An examination of the existing literature using beam theories indicates that several aspects of the vibration and buckling of rotating beams mounted off the axis of rotation were considered by several investigators (1-7). The effects of Coriolis forces on the vibration of radial rotating beams were considered in (8,9) among others. In (5), an axially prestressed, pretwisted rotating blade mounted off the axis of rotation was considered and an extended Galerkin procedure was used for solution of the equations of motion. In all other investigations

---

[1]On leave from N.B.K.R. Institute of Science & Technology, Vidyanagar-524 413, India. Presently NRC-NASA Research Associate.

cited, the beams were considered to be untwisted. Reference (1) uses a method of successive approximations, (2,3) use a perturbation technique while (7) gives asymptotic expansion formulas together with a composite expansion formula for determination of the buckling boundary of untwisted rotating blades mounted off the axis of rotation. Reference (4) uses an integrating matrix approach for the solution of untwisted blade stability analysis, while (6) unifies the rotating beam vibration analysis allowing for precone and second degree nonlinearities. From the published literature, it appears that the combined effects of pretwist, large precone, setting angle and Coriolis effects on the vibration and buckling behavior were not studied. Furthermore, greater emphasis had been laid on the solution of the governing equations of motion using various methods of solution while solutions using energy functionals have received considerably less attention.

The specific objectives of the present paper are: (1) to solve the pretwisted, preconed rotating cantilever blade vibration problem allowing for the Coriolis effects for two cases of root clamping, that is, on the axis, and off the axis of rotation, and (2) to study the effects of pretwist, precone, setting angle, Coriolis forces, and the ratio of the principal moments of inertia on the vibration frequencies and buckling boundaries. Two methods of solution are employed: (a) a finite difference procedure using second order central differences for the solution of the governing equations of motion and, (b) the total potential energy functional and the Ritz type solution using complex shape functions for the dependent variables. The present solution methods provide a positive check on the accuracy of the results for untwisted blade cases in that the finite difference procedure gives close lower bound solutions while the potential energy method gives upper bound results. Further validation of the results is accomplished by comparing the present results to closed form exact solutions wherever possible. The solution methods and parametric results provide a sufficient insight for further extensions of the present effort to account for blade sweep and second degree nonlinearities in the analysis.

FREQUENCY EQUATION BY SECOND ORDER FINITE-DIFFERENCE METHOD

The linear set of coupled bending-bending equations of motion for a torsionally rigid slender beam (Fig. 1) of rectangular cross section allowing for the effects of linear pretwist, precone and Coriolis forces can be shown (10) to be (a list of notation is given in Appendix B):

$$w^{iv}\left\{\xi\cos^2\theta+\frac{b^2}{d^2}\sin^2\theta\right\}+w'''\left\{2\gamma\xi\sin 2\theta\left(\frac{b^2}{d^2}-1\right)\right\}$$
$$+w''\left\{2\xi\gamma^2\cos 2\theta\left(\frac{b^2}{d^2}-1\right)\right\}+v^{iv}\left\{\xi\left(\frac{b^2}{d^2}-1\right)\frac{\sin 2\theta}{2}\right\}$$
$$+v'''\left\{2\gamma\xi\cos 2\theta\left(\frac{b^2}{d^2}-1\right)\right\}-v''\left\{2\gamma^2\xi\sin 2\theta\left(\frac{b^2}{d^2}-1\right)\right\}$$
$$-w\sin^2\beta_{Pc}+\frac{\ddot{w}}{\Omega^2}+\underline{\underline{\frac{2\sin\beta_{Pc}\dot{v}}{\Omega}}}$$
$$\mp w''\left\{\cos^2\beta_{Pc}\left[\bar{R}(1-\eta)\pm 0.5(1-\eta^2)\right]\right\}$$
$$\pm w'\left[\cos^2\beta_{Pc}(\bar{R}\pm\eta)\right]=0 \qquad (1)$$

$$w^{iv}\left\{\xi\left(\frac{b^2}{d^2}-1\right)\frac{\sin 2\theta}{2}\right\}+w'''\left\{2\gamma\xi\cos 2\theta\left(\frac{b^2}{d^2}-1\right)\right\}$$
$$+w''\left\{2\gamma^2\xi\sin 2\theta\left(\frac{b^2}{d^2}-1\right)\right\}+v^{iv}\left\{\xi\left(\sin^2\theta+\frac{b^2}{d^2}\cos^2\theta\right)\right\}$$
$$-v'''\left\{2\gamma\xi\sin 2\theta\left(\frac{b^2}{d^2}-1\right)\right\}-v''\left\{2\gamma^2\xi\cos 2\theta\left(\frac{b^2}{d^2}-1\right)\right\}$$
$$-v+\frac{\ddot{v}}{\Omega^2}-\underline{\underline{\frac{2\sin\beta_{Pc}\dot{w}}{\Omega}}}$$
$$\mp v''\left\{\cos^2\beta_{Pc}\left[\bar{R}(1-\eta)\pm 0.5(1-\eta^2)\right]\right\}$$
$$\pm v'\left\{\cos^2\beta_{Pc}(\bar{R}\pm\eta)\right\}=0 \qquad (2)$$

where

$$\xi=\frac{EI_{nn}}{\rho AL^4\Omega^2},\quad \theta=\varphi+\gamma\eta;\quad \eta=\frac{x}{L}\ \text{and}\ \bar{R}=\frac{R}{L} \qquad (3)$$

It may be noted that the last two terms in Eqs. (1) and (2) are shown with $\pm/\mp$ signs. For a cantilever blade case with root clamping on the periphery of a disc of radius R and the blade protruding radially outwards, the upper sign is to be taken. For the case with root clamping on the rim of a ring of radius R and the blade protruding radially inwards, the lower sign is to be assumed.

It is of interest to examine the coupled bending-bending equations and point out the various important terms arising due to the inclusion of precone. It may be seen that in Eq. (1), the term $(-w\sin^2\beta_{Pc})$ appears due to the inclusion of preconing which is a softening term. Even for the case of a rotating beam protruding radially outwards and under centrifugal tension, the effect of this term is to reduce the effective stiffness, thereby providing the mechanism for instability at reasonably large values of precone and rotational speed. It may also be noted that the Coriolis terms, which are underlined in Eqs. (1) and (2), are linear in v and w and are associated with precone. In the absence of

precone, the equations do not contain linear Coriolis forces. As could be seen in the next sections, the effect of these Coriolis terms is extremely important for blades of moderate to large thickness ratios, and also for blades possessing large pretwists.

In seeking a solution by using a finite-difference procedure, one substitutes the finite-difference expressions for the derivatives into the differential equations, for any arbitrary station j inside the beam domain. When the beam is divided into n segments, j varies from 0,1,2,.. to n; the clamped end being denoted by 0 and the free end by n. A set of n equations are written by successively assigning values for j from 1 to n. As can be seen from the expressions for the derivatives of an arbitrary variable w at the station j in terms of the second order central differences given in Appendix A, one has to eliminate the evaluation of the functions at the fictitious stations outside the beam namely w_{-2}, w_{-1}, w_{n+1}, w_{n+2}, w_{n+3}, v_{-2}, v_{-1}, v_{n+1}, v_{n+2}, and v_{n+3}. This can be accomplished by using the boundary conditions together with the recursive relations developed and discussed in detail in (11,12). These relations are also included in Appendix A for ready reference. One can thus write a set of 2n equations in terms of the variables $w_1, w_2 \ldots w_n, v_1, v_2 \ldots v_n$ for the coupled bending-bending equations of motion given by Eqs. (1) and (2) for values of $j = 1,2,\ldots n$. These equations can be represented in the following matrix form:

$$\begin{bmatrix} [\tilde{m}1] & [\tilde{0}] \\ [\tilde{0}] & [\tilde{m}2] \end{bmatrix} \begin{Bmatrix} \{\ddot{w}\} \\ \{\ddot{v}\} \end{Bmatrix} + \begin{bmatrix} [\tilde{0}] & [\tilde{C}1] \\ [-\tilde{C}1] & [\tilde{0}] \end{bmatrix} \begin{Bmatrix} \{\dot{w}\} \\ \{\dot{v}\} \end{Bmatrix} + \begin{bmatrix} [\tilde{k}1] & [\tilde{k}2] \\ [\tilde{k}3] & [\tilde{k}4] \end{bmatrix} \begin{Bmatrix} \{w\} \\ \{v\} \end{Bmatrix} = \{0\} \qquad (4)$$

where $\tilde{m}1$, $\tilde{m}2$, $\tilde{C}1$, $\tilde{k}1$, $\tilde{k}2$, $\tilde{k}3$ and $\tilde{k}4$ are square matrices of order $\tilde{n} \times \tilde{n}$ each, $\{w\}$ and $\{v\}$ are column matrices containing the vector $w_1, w_2 \ldots w_n$; $v_1, v_2 \ldots v_n$ and $\tilde{0}$ is null matrix. For brevity elements of these matrices are not presented here. Equation (4) is of the form

$$\tilde{M}\ddot{\beta} + \tilde{C}\dot{\beta} + \tilde{K}\beta = \{0\} \qquad (5)$$

Equation (5) can be written as

$$\tilde{A}\dot{x} + \tilde{B}x = 0 \qquad (6)$$

where

$$\tilde{A} = \begin{bmatrix} \tilde{0} & -\tilde{M} \\ \tilde{M} & \tilde{C} \end{bmatrix}, \quad \tilde{B} = \begin{bmatrix} \tilde{M} & \tilde{0} \\ \tilde{0} & \tilde{K} \end{bmatrix}, \quad x = \begin{Bmatrix} \dot{\beta} \\ \beta \end{Bmatrix} \qquad (7)$$

Assuming $x = x_0 e^{\lambda t}$, Eq. (6) yields

$$(\tilde{B} + \lambda\tilde{A})\, x_0 = 0 \qquad (8)$$

or

$$(\tilde{A}^* - p\tilde{B})\, x_0 = 0 \qquad (9)$$

where,

$$\tilde{A}^* = i\tilde{A},\ i = \sqrt{-1} \text{ and } p = -1/\lambda \qquad (10)$$

The eigenvalues of Eq. (9) for a conservative system are real and exist in pairs $p_1, -p_1, p_2, -p_2, \ldots p_n, -p_n$; n being the order of $\tilde{M}$, $\tilde{C}$ and $\tilde{K}$. However, eigenvectors for Eqs. (6) and (9) are the same and will occur as pairs of complex conjugate vectors (13). For instabilities, the frequency p reduces to zero (static buckling).

FREQUENCY EQUATION BY USING ENERGY FUNCTIONALS

The Lagrangian functional for a rotating, pretwisted, preconed blade including Coriolis effects but disregrading nonlinear effects can be derived from (6,10) and is given by

$$\begin{aligned} \underline{L} = L \int_0^1 \Bigg\{ & \frac{\rho A}{2}(\dot{w}^2 + \dot{v}^2) \\ & + \rho A\Omega \sin\theta_{pc}(\dot{w}v - w\dot{v}) + \frac{\rho A\Omega^2}{2}\left[v^2 + w^2 \sin^2\theta_{pc}\right] \\ & - \frac{EI_{\xi\xi}}{2L^4}\left[v''^2 \cos^2\theta + w''^2 \sin^2\theta\right] \\ & - \frac{EI_{\eta\eta}}{2L^4}\left[v''^2 \sin^2\theta + w''^2 \cos^2\theta\right] \\ & - \frac{E \sin 2\theta}{2L^4}\left(I_{\xi\xi} - I_{\eta\eta}\right) v'' w'' \mp \frac{\rho A\Omega^2 \cos^2\theta_{pc}}{2} \\ & \times \left[\bar{R}(1-\eta) \pm 0.5(1-\eta^2)\right](v'^2 + w'^2) \Bigg\} d\eta \end{aligned} \qquad (11)$$

In Eq. (11), the last term is shown with $\mp/\pm$ signs as before with the convention that the upper sign is to be taken for the cantilever blade case with root clamping on the periphery of a disc and the blade protruding outwards, while the lower sign is to be assumed for the case with root clamping on the rim of a ring and the blade protruding radially inwards.

In order to formulate the frequency equation through the Ritz process, shape functions for the variables w and v are assumed in the following complex form since the out-of-phase Coriolis effects are also included in the analysis (9):

$$w = \sum_j (A_j + iB_j) f_j e^{ipt} = \sum_j \left[(A_j \cos pt - B_j \sin pt) + i\,(A_j \sin pt + B_j \cos pt)\right] f_j \qquad (12)$$

$$v = \sum_j (C_j + iD_j) f_j e^{ipt} \qquad (13)$$

where A_j, B_j, C_j, D_j are the undetermined arbitrary real parameters in the shape functions, f_j is the polynomial function defined as

$$f_j = \frac{(j+2)(j+3)}{6}\eta^{j+1} - \frac{j(j+3)}{3}\eta^{j+2} + \frac{j(j+1)}{6}\eta^{j+3} \qquad (14)$$

The shape functions assumed here satisfy the boundary conditions

$$v = w = v' = w' = 0 \quad \text{at} \quad \eta = 0 \quad \text{and}$$

$$v'' = w'' = v''' = w''' = 0 \quad \text{at} \quad \eta = 1 \qquad (15)$$

The real and imaginary parts of the shape functions are substituted into the Lagrangian functional separately, the indicated integrations are performed, the resulting functional is time averaged in the traditional manner and the Ritz process is applied by minimizing the resulting Lagrangian functional, that is

$$\frac{\partial \bar{L}}{\partial A_j} = 0, \quad \frac{\partial \bar{L}}{\partial B_j} = 0, \quad \frac{\partial \bar{L}}{\partial C_j} = 0, \quad \frac{\partial \bar{L}}{\partial D_j} = 0, \quad j = 1,2,\ldots k \qquad (16)$$

The resulting equations can be written in the following form of the eigenvalue problem after transformations similar to those described in the previous section are made:

$$\underset{\sim}{C} + p\underset{\sim}{D} = 0 \qquad (17)$$

Where $\underset{\sim}{C}$ and $\underset{\sim}{D}$ are complex matrices.

RESULTS AND DISCUSSION

The eigenvalue problems defined by Eqs. (9) and (17) were solved by using computer programs developed in FORTRAN language. These programs were run on IBM and CRAY computers at the NASA Lewis Research Center. Use was made of standard eigenvalue extraction routines (14), and a 15-point Gaussian quadrature formula for carrying out integrations where necessary. Results thus generated are presented and discussed in what follows.

CONVERGENCE

The relative convergence rates produced by the finite-difference method using second order central differences, and the potential energy method were obtained for several configurations of rotating blade cases. A typical set of such results are presented in Table I for the case of a preconed, rotating beam, including Coriolis effects. From the convergence pattern shown in Table I, it can be seen that the potential energy method produces convergence to seven significant figures with an eight-term solution ($k = 8$) while the finite-difference method produces the lowest five frequencies to within 0.05 percent error when the beam is divided into 30 segments ($n = 30$), although the convergence is up to four significant figures. It is worth noting here that the convergence resulting from the present formulation of the finite-difference procedure making use of second order central differences is much more rapid than a solution that could be obtained by the classical finite-difference method. It has been established (12,15) that this second order finite-difference method is computationally more efficient than the classical approaches of solving the equations of motion using ordinary finite-difference procedures. Further, the Richardson's extrapolation procedure (16,17) can be applied for frequencies obtained with two or three different matrix sizes to improve the accuracy while keeping the matrix sizes small in the finite-difference methods.

When a comparison of the present converged results is made to those presented by Leissa and Co (9) for the specialized simple case presented in Table I, it is observed that present results show excellent agreement with those of (9). The Ritz method of solution was employed in (9) making use of a different form of shape functions. Further, the extensional deformation was taken into account in (9) while the present work treats the blades to be extensionally rigid. It is thus evident from the close agreement of the present results with those of (9) that for the geometric and physical parameters considered in this work, the extensional deformation can safely be ignored. Exclusion of this additional degree of freedom reduces the number of equations of motion and the consequent computational space and time.

Finally, for all the vibration and stability problems reported in this work, solutions were obtained by using the upper bound potential energy method with $k = 8$, and the usually lower bound finite-difference method with $n = 30$. In view of the close agreement between these two sets of results observed (of the order of 0.05 percent difference), only one set of results are presented in what follows for brevity.

VIBRATION AND STABILITY OF ROTATING BLADES

In order to study the effects of pretwist, precone, Coriolis forces and thickness ratio (d/b) on the natural frequencies of rotating blades, several cases of twisted, rotating blades were solved. Typical cases of thickness ratio that approximately represent propeller blades ($d/b = 0.5$ or 0.25), and advanced turboprop blades ($d/b = 0.05$) were considered for a typical aspect ratio (L/b) of 5. The dimensionless rotational speed (Ω/ω_1) (where Ω and ω_1 are respectively the rotational speed, and the uncoupled fundamental bending frequency of the blade) was varied. Typical set of such results are presented in Table II to IV, and in Figs. 2 and 3. Table V is prepared using the results presented in Tables III and IV to illustrate the effect of Coriolis forces on a typical preconed blade. It may be noted that R is set equal to zero in these calculations for simplicity.

The effect of pretwist on nonrotating blade frequencies predicted by beam theories is well understood in the published literature. The frequencies presented in Table II for $\Omega/\omega_1 = 0$ case agree well with those existing in the literature, and exhibit the well established coupling trends (18-20). The fundamental mode frequency is seen to increase slightly with increasing pretwist, consistent with the inherent quality of the beam theory (21). However, for rotating pretwisted blades it can be seen that the fundamental mode frequency shows a decreasing trend for increasing pretwist beyond certain values of Ω/ω_1.

The effect of rotation on the coupling trends of pretwisted blades is illustrated in Table II. For pretwisted blades with thickness ratio greater than 0.1596, the second coupled mode will be closer to the fundamental uncoupled mode in chordwise direction while the third coupled mode will be closer to the uncoupled second mode frequency in the flapwise direction. The effect of pretwist for such blades is to couple the second mode uncoupled flapwise frequency and the fundamental chordwise frequency in such a way that the lower frequency is reduced and the higher one is increased with increasing pretwists. This important coupling trend observed

for nonrotating pretwisted blades does not necessarily hold for rotating blades. This may be verified from the results presented in Table II for pretwisted blade cases with thickness ratio of 0.5 and rotational speed parameter values of 3 and greater. The reason for the change in the coupling trend is that although the coupled frequencies are raised by the rotation induced centrifugal forces, not all the modes are stiffened in a proportional manner.

Next, the effects of pretwist and precone on rotating blade frequencies are considered. Some typical results are presented in Table III neglecting Coriolis effects, and in Table IV including Coriolis effects. Futher results presented in Table V indicate the effect of Coriolis forces, those in Fig. 2 indicate the effect of pretwist, and those in Fig. 3 indicate the effect of precone in a parametric form. The following observations are made from the results presented:

(1) For small precone angles and small pretwists, an increase in the rotational speed increases the frequencies of all modes. For large precone angles, the frequencies of pretwisted or untwisted blade increase in a nonlinear manner up to a certain value of the rotational parameter, Ω/ω_1, beyond which a decreasing trend is observed. At some value of the rotational parameter Ω/ω_1, for a given thickness ratio and precone, the fundamental mode frequency becomes zero indicating static instability. A detailed discussion on this phenomenon for untwisted blades was presented in (6,22). This instability occurs over a zone of Ω/ω_1 values indicating an instability band, beyond which the blade becomes stable again. This can be verified by referring to Table IV for precone angles of 60° and 90° of large thickness ratio blade cases. By comparing the results with and without Coriolis effects presented in Tables III and IV respectively, it can be seen that the Coriolis effects change the onset and width of the instability band for large thickness ratio blade cases. However, the Coriolis effects appear to be not so significant for small thickness ratio blade cases operating at low rotational speeds.

(2) The effect of precone in the absence of Coriolis effects can be seen by comparing the results presented in Tables II and III. From these tables, it can be seen that the frequencies of all modes decrease as the precone is increased, at a given rotational speed for all thickness ratios and pretwists. For smaller rotational speeds, the blades are stable for all precone angles. For Ω/ω_1 values of one and greater, instabilities could occur over a zone of precone angles depending on the pretwist and thickness ratio. However, inclusion of Coriolis effects makes these frequency variations somewhat different. This fact can be verified by a mutual comparison of the results presented in Tables III and IV for a 30° pretwisted blade with $\Omega/\omega_1 = 3$. It can be seen that for large thickness ratio blades with d/b = 0.5, the instability band starts for precone angles greater than 45°, and extends up to 90° when the Coriolis effects are ignored while the instability band is restricted to between 47° and 50° when the Coriolis effects are included.

(3) In order to provide a clearer insight into the Coriolis effects, the percentage variations of the frequency ratios were calculated from the results presented in Tables III and IV for a typical precone angle of 45°. These results are presented in Table V. It can be seen from these results that the effect of Coriolis forces becomes more significant as the rotational speed is increased. The fundamental mode frequency shows a decreasing trend when the Coriolis forces are included while the higher mode frequencies show both increasing and decreasing trends. For large thickness ratio blades, the Coriolis effects produce large frequency ratio variations even for low rotational speeds. Significant frequency ratio variations occur for the first and the second modes of untwisted blades, and even for higher modes for pretwisted blades. The Coriolis effects are important even for low thickness ratio blades for high rotational speeds, particularly when pretwist is present.

(4) The effect of varying pretwist for a given thickness ratio and precone angle are presented in Fig. 2. Specifically, for $\beta_{pc} = 45°$ and thickness ratio of 0.25, the semi-indefinite instability band starts at a Ω/ω_1 value somewhere between 5.7 to 5.8 for a 60° pretwisted blade while such an instability band starts at a Ω/ω_1 value somewhere between 5.1 to 5.2 for a 90° pretwisted blade. For small thickness ratio blades with d/b = 0.05 and $\beta_{pc} = 45°$, instability starts at $27.5 \leq \Omega/\omega_1 \leq 28.0$ for $\gamma = 60°$, and at $23.0 \leq \Omega/\omega_1 \leq 23.5$ for $\gamma = 90°$. For $\beta_{pc} = 60°$, d/b = 0.05, instability starts at $1.48 \leq \Omega/\omega_1 \leq 1.49$ for blades of 0° or 30° pretwist. For $\beta_{pc} = 90°$, d/b = 0.05 and $\gamma = 0°$ blade case, instability starts at $\Omega/\omega_1 = 1.0$, while for the same blade with 30° pretwist, instability occurs at $1.003 \leq \Omega/\omega_1 \leq 1.004$. These observations reveal that an increase in pretwist can either increase or decrease the rotational speed to cause instability depending on whether the precone is lesser or greater than 45° respectively.

(5) The effect of increasing the precone angle for low thickness ratio pretwisted blade case is shown in Fig. 3. It can be seen from this figure that considerable change in the slopes of the curves occurs for precone angles greater than 45°.

From the foregoing discussion, it may be concluded that the Coriolis effects associated with precone angle may be neglected for low thickness ratio blades subjected to low rotational speeds. Since the advanced turboprop blades possess low thickness ratios, and operate around speeds of the order of $\Omega/\omega_1 = 1$, it appears logical to disregard the Coriolis effects associated with precone. However, it is essential to retain the Coriolis effects when pretwists of larger magnitude are present for the blades operating even at low rotational speeds.

BUCKLING OF ROTATING BLADES MOUNTED OFF THE AXIS OF ROTATION

A geometric arrangement giving rise to rotationally induced radial forces which are compressive rather than tensile is shown in Fig. 4. Such rotating beams without pretwist and precone have been analyzed for specialized cases of inplane vibration ($\varphi = 90°$) or out-of-plane vibrations ($\varphi = 0°$) extensively (1-7). For a beam even without pretwist and precone, the flapwise and lagwise bending motions are coupled for setting angles other than 0° and 90°. The purpose of this section is to re-examine the buckling behavior of rotating beams in the presence of pretwist, precone and Coriolis forces using the coupled bending-bending equations given earlier.

An examination of the published work reveals that most of the problems in the different analytical

approaches were due to some convergence problems of the solution procedure adopted. These were overcome by alternative solution methods (4) or by making use of certain expansion formulae (7). To ascertain that the present numerical procedures do not exhibit similar drawbacks as were observed in the existing works, specialized simple cases were solved first, comparisons of present results were made to existing standard values, and accuracies of present theoretical developments were established. As a typical example, the closed form solution obtained in (2) for the case of buckling out of the plane of rotation ($\varphi = \gamma = \beta_{pc} = 0$) gives a value of $\Omega/\lambda_1 = 5.6746$ for $\bar{R} = 1.0$. Present solution with the potential energy method gives the values of Ω/λ_1 for $\bar{R} = 1$ as 5.6912, 5.6753, and 5.6747 for $k = 2$, 3 and 4, respectively. For $k = 8$ or 9, this value converges to 5.67468. The finite-difference procedure produces a value which is about 0.06 percent off this exact value. Further, the buckling boundaries for in-plane and out-of-plane vibration cases plotted in Fig. 5(a) agree very closely with those obtained by using the integrating matrix method (4).

A parametric study was made to study the effects of pretwist, setting angle and thickness ratio (d/b) on the buckling boundary. Results of this investigation are presented in graphical form in Figs. 5(b) to (d) for $d/b = 0.25$, and in Figs. 6(a) to (c) for $d/b = 0.05$. From the results presented, the following observations can be made:

1. When the blade thickness ratio is small, or the ratio of the principal second moments of area is large, the stability boundaries of pretwisted blades for $\varphi = 0^\circ$ and 90° follow closely those for untwisted blades.

2. An increase in the pretwist angle for a given value of setting angle φ moves the stability boundary towards left. That is, for a given rotational speed, buckling occurs at a lower value of $\bar{R}$ for increasing γ at a given φ.

3. An increase in the setting angle φ for a given pretwist has similar effect as discussed in (2) above.

4. For nonzero pretwist, all curves tend to meet at $\bar{R} = 0$ as the rotational parameter, Ω/λ_1, tends to infinity.

5. For large values of d/b, there is a marked change in the stability boundary. Comparing $\varphi = 0^\circ$, $\gamma = 15^\circ$ curve with $\varphi = 0^\circ$, $\gamma = 0^\circ$ curve presented in Fig. 5(a), one observes that the former closely follows the latter up to a low value Ω/λ_1 and detaches from this path to rapidly reduce the value of $\bar{R}$ for increasing values of Ω/λ_1. As the pretwist angle is increased, this phenomenon becomes more pronounced.

The effects of precone, pretwist and Coriolis forces on the critical speed for causing instability are presented in Tables VI and VII. From these limited sets of results, it appears that the critical speed for causing buckling for a given value $\bar{R}$ decreases very rapidly as the precone is increased for values of $\bar{R}$ up to about 1.2. Beyond this value of $\bar{R}$, there is a slight gain in the critical speed to cause instability as the precone is increased from 0°. The inclusion of Coriolis effects in the analysis decreases the value of $\bar{R}$ at a given rotational speed to cause instability generally. As this critical speed is increased further, the effect of the Coriolis terms decreases. The nonlinear effects may be more important in such cases rather than the Coriolis terms. The effect of nonlinear terms were studied in (6) for simple cases of preconed beam vibration. It was observed that approximately 6 percent decrease in the frequency value occurs for first flapwise bending frequency, and about 30 percent increase in the first lagwise frequency for an untwisted, 15° preconed beam with $d/b = 1$ and $\Omega/\omega_1 = 3.2$ due to the steady state deformation induced by the nonlinear terms. From these observations, it appears that inclusion of nonlinear terms and the Coriolis effects into the analysis is imperative. Finally, the effect of increasing pretwist, shown in Table VII, reveals that for buckling to occur at a given critical speed, the value of $\bar{R}$ may either increase or decrease.

CONCLUSIONS

Parametric studies were conducted to ascertain the individual and collective effects of pretwist, precone, setting angle, Coriolis forces and blade thickness ratio on the vibration frequencies and buckling boundaries of rotating beams. Two methods of solution for studying blade vibration and stability were used, namely, a finite difference procedure based upon second-order central differences that usually produces close lower bound solutions, and the potential energy method that produces close upper bound solutions. Results obtained by using these two methods were found to be in excellent agreement. Further validation of the present results was accomplished by comparisons to results in the literature for specialized simple cases.

The parametric results show that the inclusion of Coriolis effects is necessary for blades of moderate to large thickness ratios while these effects are not so important for small thickness ratio blades. Thus, the linear Coriolis terms associated with precone may be neglected in the dynamic analysis of advanced turboprop blades. However, the effect of Coriolis terms in the presence of second degree nonlinear terms is yet to be assessed. For a given thickness ratio and pretwist, an increase in rotational speed has a destabilizing effect for large precone angles. For a given thickness ratio and aspect ratio, an increase in pretwist angle has a stabilizing effect for precone angle less than 45°, and a destabilizing effect for precone angles greater than 45°. For a beam mounted off the axis of rotation, the pretwist and setting angle have a significant influence on rotation-induced buckling instability. However, this influence depends markedly on the blade thickness ratio.

The parametric results presented in this work are believed to be useful for future comparisons of theoretical solutions including sweep and nonlinear effects, and thereby ascertaining the importance of these complicating effects.

APPENDIX A
FINITE-DIFFERENCE EQUATIONS FOR DERIVATIVES

The finite-difference expressions for the derivatives of an arbitrary functional $\psi(\eta)$ in terms of second order central differences are given as follows for an arbitrary station j:

$$\psi_j' = \left[\psi_{j-2} - 8\psi_{j-1} + 8\psi_{j+1} - \psi_{j+2}\right] \Big/ 12h \qquad (A1)$$

$$\psi_j'' = \left[-\psi_{j-2} + 16\psi_{j-1} - 30\psi_j + 16\psi_{j+1} - \psi_{j+2}\right] \Big/ 12h^2 \qquad (A2)$$

$$\psi_j''' = \left[\psi_{j-3} - 8\psi_{j-2} + 13\psi_{j-1} - 13\psi_{j+1} + 8\psi_{j+2} - \psi_{j+3}\right] \Big/ 8h^3 \qquad (A3)$$

$$\psi_j^{iv} = \left[-\psi_{j-3} + 12\psi_{j-2} - 39\psi_{j-1} + 56\psi_j - 39\psi_{j+1} + 12\psi_{j+2} - \psi_{j+3}\right] \Big/ 6h^4 \qquad (A4)$$

Equations (A1) to (A4) are applicable for a beam divided into n number of segments of equal length and η is the nondimensional length coordinate varying from $\eta = 0$ at root section to $\eta = 1$ at free end for a cantilever beam. Thus $h = 1/n$.

The boundary conditions for a cantilever beam under coupled bending-bending motion are

$$v = w = v' = w' = 0 \quad \text{at} \quad \eta = 0 \qquad (A5)$$

$$v'' = w'' = v''' = w''' = 0 \quad \text{at} \quad \eta = 1 \qquad (A6)$$

Using the expressions for the derivatives given by Eqs. (A1) to (A3) and invoking the conditions of symmetry as discussed in (15), one can write the following recursive relations which satisfy the boundary conditions for suitably large n:

$$w_{n+1} - w_{n-1} = 2(w_n - w_{n-1}); \quad v_{n+1} - v_{n-1} = 2(v_n - v_{n-1}) \qquad (A7)$$

$$w_{n+2} - w_{n-2} = 4(w_n - w_{n-1}); \quad v_{n+2} - v_{n-2} = 4(v_n - v_{n-1}) \qquad (A8)$$

$$w_{n+3} - w_{n-3} = 6(w_n - w_{n-1}); \quad v_{n+3} - v_{n-3} = 6(v_n - v_{n-1}) \qquad (A9)$$

$$w_{-1} = w_1, \; w_{-2} = w_2, \; v_{-1} = v_1, \; v_{-2} = v_2 \qquad (A10)$$

Equations (A7) to (A10) can be used to eliminate the fictitious stations outside the beam domain.

APPENDIX B
NOMENCLATURE

A	area at any section
$\underset{\sim}{A}, \underset{\sim}{B}, \underset{\sim}{C}, \underset{\sim}{M}, \underset{\sim}{K}$, etc.	matrices
A_j, B_j, C_j, D_j	arbitrary parameters in shape functions
b, a	breadth and thickness of blade
d/b	thickness ratio
E	Young's modulus
f_j	shape function
h	length of each elemental beam segment
$I_{\eta\eta}, I_{\xi\xi}$	area moments of inertia about major and minor principal centroidal axes, respectively
J	dummy index
k	number of terms in assumed solution
L	length of beam
$\underline{L}$	time averaged value of the Lagrangian functional
n	number of beam segments
p	natural radian frequency
R	radius of disc
$\bar{R}$	nondimensional radius, R/L
t	time
v	displacement in the chordwise direction
w	displacement in the flapwise direction
x	running coordinate along longitudinal x-axis
β_{pc}	precone angle (The angle the blade centerline makes with the plane of rotation, see Fig. 1).
γ	pretwist of the blade over length L
ρ	mass density of blade material
ω_1	exact fundamental mode frequency of straight beam, $3.51602\ \lambda_1$
Ω	rotational speed, radians/sec
θ	geometric pitch angle, $(\varphi + \gamma\eta)$
φ	stagger angle (collective pitch, the rotation of the blade root chord about the blade axis)
η	nondimensional length coordinate, x/L
ξ	nondimensional rotational parameter, $EI_{\eta\eta}/\rho AL^4\Omega^2$
λ_1	frequency parameter, $\sqrt{EI_{\eta\eta}/\rho AL^4}$
$(\dot{})$	dot over a parameter represents time derivative, $\partial/\partial t$
$(\,)'$	prime denotes differentiation with respect to η, $\partial/\partial\eta$

REFERENCES

1. Mostaghel, N., and Tadjbakhsh, I., "Buckling of Rotating Rods and Plates," International Journal of Mechanical Sciences, Vol. 15, No. 6, 1973, pp. 429-434.

2. Lakin, W.D., and Nachman, A., "Unstable Vibrations and Buckling of Rotating Flexible Rods," Quarterly of Applied Mathematics, Vol. 35, No. 4, Jan. 1978, pp. 479-493.
3. Lakin, W.D., and Nachman, A., "Vibration and Buckling of Rotating Flexible Rods at Transitional Parameter Values," Journal of Engineering Mathematics, Vol. 13, 1979, pp. 339-346.
4. White, W.F. Jr., Kvaternik, R.G., and Kaza, K.R.V., "Buckling of Rotating Beams," International Journal of Mechanical Sciences, Vol. 21, No. 12, 1979, pp. 739-745.
5. Wang, J.T.S., "On the Buckling of Rotating Rods," International Journal of Mechanical Sciences, Vol. 18, No. 7-8, 1976, pp. 407-411.
6. Kvaternik, R.G., White W.F., and Kaza, K.R.V., "Nonlinear Flap-Lag-Axial Equations of a Rotating Beam with Arbitrary Precone Angle," AIAA Paper, 78-491, 1978.
7. Peters, D.A., and Hodges, D.H., "In-Plane Vibration and Buckling of a Rotating Beam Clamped Off the Axis of Rotation," Journal of Applied Mechanics, Vol. 47, No. 2, June 1980, pp. 398-402.
8. Sreenivasamurthy, S., and Ramamurti, V., "Coriolis Effect on the Vibration of Flat Rotating Low Aspect Ratio Cantilever Plates," Journal of Strain Analysis, Vol. 16, No. 2, Apr. 1981, pp. 97-106.
9. Leissa, A., and Co, C., "Coriolis Effects on the Vibrations of Rotating Beams and Plates," Proceedings XII SECTAM Conference, Vol. II, Auburn Univ., AL, 1984, pp. 508-513.
10. Kaza, K.R.V., and Kvaternik, R.G., "Nonlinear Aeroelastic Equations for Combined Flapwise Bending, Chordwise Bending, Torsion, and Extension of Twisted Nonuniform Rotor Blades in Forward Flight," NASA TM-74059, 1977.
11. Subrahamanyam, K.B., and Kaza, K.R.V., "An Improved Finite-Difference Analysis of Uncoupled Vibrations of Tapered Cantilever Beams," NASA TM-83495, 1983.
12. Subrahamanyam, K.B., and Kaza, K.R.V., "Improved Methods of Vibration Analysis of Pretwisted Airfoil Blades," NASA TM-83735, 1984.
13. Gupta, K.K., "Free Vibration Analysis of Spinning Structural Systems," International Journal for Numerical Methods in Engineering Vol. 5, No. 3, Jan. - Feb. 1973, pp. 395-418.
14. The International Mathematical and Statistical Library (IMSL), Houston, Texas, 1975.
15. Subrahamanyam, K.B., and Kaza, K.R.V, "An Improved Finite-Difference Vibration Analysis of Pretwisted, Tapered Beams," Proceedings of the XII Southeastern Conference, Vol. I, Auburn Univ., AL, 1984, pp. 118-126.
16. Richardson, L.F., "The Approximate Arithmetical Solution by Finite Differences of Physical Problems Involving Differential Equations, With an Application to the Stresses in a Masonry Dam," Philosophical Transactions, Royal Society of London, Series A, Vol 210, 1911, pp. 307-357.
17. Salvadori, M.G., "Numerical Computation of Buckling Loads by Finite Differences," Proceedings of the American Society of Civil Engineers, Vol. 75, No. 10, Dec. 1949, pp. 1441-1475.
18. Subrahmanyham, K.B., Kulkarni, S.V., and Rao, J.S., "Application of the Reissner Method to Derive the Coupled Bending-Torsion Equations of Dynamic Motion of Rotating Pretwisted Cantilever Blading with Allowance for Shear Deflection, Rotary Inertia, Warping and Thermal Effects," Journal of Sound and Vibration, Vol. 84, No. 2, Sept. 22, 1982, pp. 223-240.
19. Dokumaci, E., Thomas, J., and Carnegie, W., "Matrix Displacement Analysis of Coupled Bending-Bending Vibrations of Pretwisted Blading," Journal of Mechanical Engineering Science, Vol. 9, No. 4, Oct. 1967, pp. 247-254.
20. Rosard, D.D., "Natural Frequencies of Twisted Cantilever Beams," ASME Journal of Applied Mechanics, Vol. 20, No. 2, June 1953, pp. 241-244.
21. Leissa, A.W., Macbain, J.C., and Kielb, R.E, "Vibration of Twisted Cantilever Plates-Summary of Previous and Current Studies," Journal of Sound and Vibration, Vol. 96, No. 2, Sept. 22, 1984, pp. 159-173.
22. Kaza, K.R.V., "Rotation in Vibration, Optimization, and Aeroelastic Stability Problems," Ph.D. Dissertation, Stanford University, 1974. (also NASA CR-138295)

TABLE I. - CONVERGENCE PATTERN OF FREQUENCY RATIOS (p/λ_1) OF A PRECONED, ROTATING BEAM INCLUDING CORIOLIS EFFECTS

$$\left[\frac{\Omega}{\omega_1} = 0.5,\ \beta_{p_c} = 30^\circ,\ d/b = 0.5,\ L/d = 20,\ \gamma = \bar{R} = 0.\right]$$

(a) Second order finite-difference method (lower bound)

Setting angle, φ	Mode number	n = 6	n = 10	n = 12	n = 15	n = 18	n = 20	n = 25	n = 30
	1	3.62676	3.63274	3.63349	3.63400	3.63423	3.63435	3.63446	3.63453
	2	7.29213	7.30161	7.30273	7.30349	7.30382	7.30396	7.30412	7.30416
0°	3	21.8375	22.2268	22.2715	22.3011	22.3144	22.3182	22.3247	22.3272
	4	43.2818	44.0482	44.1355	44.1929	44.2178	44.2269	44.2390	44.2459
	5	57.6280	61.0874	61.4944	61.7596	61.8704	61.9180	61.9679	61.9892

(b) Potential energy method (upper bound)

Setting angle, φ	Mode number	k = 1	k = 2	k = 3	k = 4	k = 5	k = 6	k = 7	k = 8 or k = 9
	1	3.643190	3.634715	3.634639	3.634639	3.634639	3.634639	3.634639	3.634639
	2	7.328086	7.304394	7.304332	7.304331	7.304331	7.304331	7.304331	7.304331
0°	3	--------	23.00084	22.33244	22.33243	22.33158	22.33158	22.33158	22.33158
	4	--------	45.60155	44.25278	44.25276	44.25100	44.25099	44.25099	44.25099
	5	--------	---------	66.57146	62.08343	62.05877	62.01729	62.01712	62.01699

TABLE II. – EFFECT OF ROTATION UPON THE FREQUENCY RATIOS, p/λ_1, OF PRETWISTED CANTILEVER PLATES

$\varphi = 0$, $\bar{R} = 0$, $\theta_{PC} = 0$

$\frac{\Omega}{\omega_1}$	Mode number	d/b = 0.5				d/b = 0.25				d/b = 0.05			
		γ = 0	γ = 30	γ = 60	γ = 90	γ = 0	γ = 30	γ = 60	γ = 90	γ = 0	γ = 30	γ = 60	γ = 90
0	1	3.5160	3.5245	3.5496	3.5900	3.5160	3.5266	3.5580	3.6088	3.5160	3.5273	3.5607	3.6149
	2	7.0320	6.9585	6.7595	6.4847	14.064	13.133	11.467	9.9596	22.034	19.646	15.651	12.535
	3	22.034	22.339	23.210	24.531	22.034	23.669	27.317	31.651	61.695	58.233	53.169	47.697
	4	44.068	42.896	40.306	37.457	61.695	58.677	52.947	47.613	70.320	80.703	97.141	99.068
	5	61.695	63.423	67.627	72.973	88.137	92.559	101.56	104.62	120.919	120.304	123.379	144.268
0.5	1	4.0049	4.0082	4.0183	4.0354	4.0049	4.0103	4.0267	4.0543	4.0049	4.0110	4.0293	4.0602
	2	7.0742	7.0064	6.8227	6.5692	14.085	13.201	11.583	10.097	22.484	20.038	15.958	12.783
	3	22.484	22.780	23.627	24.917	22.484	24.062	27.643	31.930	62.141	58.631	53.551	48.055
	4	44.260	43.108	40.551	37.730	62.141	59.081	53.306	47.945	70.325	80.782	97.343	99.420
	5	62.141	63.847	68.016	73.333	88.233	92.693	101.75	104.96	121.378	120.745	123.692	144.427
1.0	1	5.1916	5.1824	5.1552	5.1120	5.1916	5.1876	5.1761	5.1583	5.1916	5.1887	5.1804	5.1680
	2	7.1969	7.1461	7.0096	6.8250	14.148	13.384	11.897	10.480	23.783	21.167	16.842	13.499
	3	23.783	24.055	24.839	26.041	23.783	25.217	28.606	32.759	63.457	59.798	54.676	49.111
	4	44.830	43.735	41.273	38.533	63.457	60.276	54.362	48.923	70.337	81.023	97.933	100.461
	5	63.457	65.103	69.171	74.400	88.520	93.098	102.32	105.94	122.744	122.059	124.639	144.906
3.0	1	8.2496	8.2156	8.1195	7.9774	11.7400	11.703	11.570	11.267	11.740	11.725	11.674	11.571
	2	11.740	11.749	11.772	11.804	14.780	14.504	13.849	13.170	34.699	30.466	24.069	19.334
	3	34.699	34.834	35.233	35.872	34.699	35.502	37.704	40.780	70.473	70.065	65.224	59.067
	4	50.514	49.804	48.078	46.044	75.952	71.242	64.064	57.993	75.952	84.242	103.103	110.388
	5	75.952	77.191	80.470	84.936	91.530	97.572	108.17	115.07	136.354	135.234	134.979	150.095
5.0	1	9.6262	9.6137	9.5774	9.5203	15.861	15.702	15.274	14.682	18.706	18.693	18.643	18.529
	2	18.707	18.709	18.714	18.723	18.707	18.730	18.782	18.836	49.635	42.280	33.218	26.820
	3	49.635	49.637	49.658	49.742	49.635	50.111	51.481	53.528	70.742	80.115	81.216	74.586
	4	60.266	59.896	58.962	57.827	95.733	86.492	78.111	71.573	95.733	96.286	110.842	125.094
	5	95.733	96.623	99.085	102.598	97.271	107.45	119.49	128.98	159.683	157.988	154.907	161.384

TABLE III. – EFFECT OF ROTATION UPON THE FREQUENCY RATIOS, p/λ_1, OF PRETWISTED, PRECONED BLADES NEGLECTING CORIOLIS EFFECTS

$\psi = 0$, $\bar{R} = 0$

Thickness a/b ratio	γ, degree	$\frac{\Omega}{\omega_1}$	Mode number	$\beta_{PC} = 15°$	$\beta_{PC} = 30°$	$\beta_{PC} = 45°$	$\beta_{PC} = 60°$	$\beta_{PC} = 90°$
0.50	0	0.5	1	3.9480	3.7897	3.5576	3.3111	3.0450
			2	7.0567	7.0088	6.9427	6.8760	6.8067
			3	22.450	22.355	22.225	22.095	21.964
		1.0	1	5.0155	4.4986	3.6751	2.5996	Unstable
			2	7.1283	6.9371	6.6669	6.3849	6.0699
			3	23.652	23.291	22.789	22.276	21.752
		3.0	1	7.7133	6.0017	1.9294	Unstable	Unstable
			2	11.055	8.9112	4.5417	Unstable	Unstable
			3	33.892	31.578	28.103	24.124	19.345
0.50	30	0.5	1	3.9516	3.7925	3.5637	3.3189	3.0548
			2	6.9884	6.9390	6.8709	6.8022	6.7328
			3	22.746	22.653	22.526	22.398	22.269
		1.0	1	5.0072	4.4931	3.6738	2.6047	0.24471
			2	7.0755	6.8788	6.6005	6.3097	6.0049
			3	23.926	23.571	23.078	22.574	22.060
		3.0	1	7.6748	5.9420	1.6216	Unstable	Unstable
			2	11.064	8.9271	4.6029	Unstable	Unstable
			3	34.034	31.742	28.305	24.380	19.691
0.25	30	0.5	1	3.9537	3.7946	3.5658	3.3211	3.0572
			2	13.189	13.155	13.109	13.062	13.014
			3	24.032	23.948	23.833	23.718	23.603
		1.0	1	5.0121	4.4970	3.6769	2.6079	0.27314
			2	13.338	13.210	13.031	12.845	12.653
			3	25.099	24.774	24.324	23.860	23.406
		3.0	1	11.020	8.8796	4.5028	Unstable	Unstable
			2	14.180	13.247	11.822	10.117	7.8232
			3	34.721	32.492	29.180	25.463	21.188
0.05	30	0.5	1	4.5376	4.1767	3.6255	2.9727	2.1283
			2	20.556	20.342	20.047	19.748	19.443
			3	59.171	58.976	58.707	58.437	58.165
		1.0	1	5.0131	4.4979	3.6778	2.6089	0.2816
			2	21.049	20.723	20.269	19.804	19.329
			3	59.688	59.387	58.971	58.551	58.127
		3.0	1	11.039	8.8937	4.5152	Unstable	Unstable
			2	29.759	27.720	25.619	21.009	16.574
			3	69.373	67.634	64.336	60.976	57.270

TABLE IV. - EFFECT OF ROTATION UPON THE FREQUENCY RATIOS, p/λ_1, OF PRECONED BLADES INCLUDING CORIOLIS EFFECTS.

$\varphi = 0$, $\bar{R} = 0$

Thickness c/b ratio	γ, degree	$\frac{\Omega}{\omega_1}$	Mode number	$\theta_{pc} = 15°$	$\theta_{pc} = 30°$	$\theta_{pc} = 45°$	$\theta_{pc} = 60°$	$\theta_{pc} = 90°$
0.50	0	0.5	1	3.9015	3.6346	3.2951	2.9719	2.6558
			2	7.1408	7.3043	7.4956	7.6607	7.8064
			3	22.443	22.332	22.179	22.025	21.872
		1.0	1	4.7452	3.8423	2.8358	1.8415	Unstable
			2	7.5342	8.1221	8.6401	9.0132	9.2225
			3	23.625	23.193	22.599	21.999	21.396
		3.0	1	6.5731	3.6629	.55818	2.0659	4.8405
			2	12.972	14.599	15.694	16.276	16.153
			3	33.533	30.433	26.237	21.871	17.040
0.50	30	0.5	1	3.9039	3.6354	3.2950	2.9718	2.6566
			2	7.0739	7.2389	7.4311	7.5963	7.7416
			3	22.739	22.628	22.476	22.324	22.172
		1.0	1	4.7323	3.8276	2.8230	1.8346	.15902
			2	7.4865	8.0744	8.5890	8.9573	9.2407
			3	23.898	23.467	22.877	22.283	21.685
		3.0	1	6.5469	3.6354	.47607	2.0902	4.9093
			2	12.9698	14.588	15.669	16.114	15.773
			3	33.658	30.547	26.363	22.049	17.563
0.25	30	0.5	1	3.9439	3.7599	3.5016	3.2331	2.9510
			2	13.221	13.274	13.344	13.409	13.472
			3	24.032	23.947	23.831	23.716	23.600
		1.0	1	4.9607	4.3345	3.4286	2.3587	.24012
			2	13.474	13.697	13.955	14.168	14.342
			3	25.097	24.765	24.310	23.855	23.402
		3.0	1	9.7489	6.5659	2.7641	Unstable	Unstable
			2	16.025	17.893	19.162	19.519	17.773
			3	34.648	32.253	28.[illegible]7	25.360	22.970
0.05	30	0.6	1	4.5343	4.1653	3.6054	2.9478	2.1043
			2	20.568	20.386	20.135	19.879	19.619
			3	59.174	59.083	58.723	58.460	58.195
		1.0	1	5.0075	4.4791	3.6466	2.5752	0.2767
			2	21.067	20.791	20.405	20.008	19.600
			3	59.692	59.399	58.595	58.586	58.175
		3.0	1	10.963	8.6803	4.2661	Unstable	Unstable
			2	29.905	28.251	25.651	22.528	18.571
			3	69.419	67.514	64.593	61.315	57.679

TABLE V. - PERCENTAGE VARIATION OF FREQUENCY RATIOS* DUE TO CORIOLIS EFFECTS

$\varphi = 0$, $\bar{R} = 0$, $L/b = 5$, $\beta_{Pc} = 45^\circ$

Thickness ratio d/b	$\frac{\Omega}{\omega_1}$	$\gamma = 0^\circ$			$\gamma = 30^\circ$		
		I mode	II mode	III mode	I mode	II mode	III mode
0.50	0.5	-7.379	7.964	-0.207	-7.540	8.153	-0.222
	1.0	-22.837	29.597	-0.834	-23.159	30.127	-8.710
	3.0	-71.070	245.553	-6.640	-70.642	240.416	-6.861
0.05	1.0	-0.250	-0.004	0.002	-0.848	0.671	0.041
	3.0	-2.200	-0.064	-0.006	-5.517	4.192	0.400
	5.0	-5.851	-0.208	6.254	-10.850	7.816	1.679

*Percentage variation = $(FR_C - FR_{NC}) * 100/FR_{NC}$
FR_{NC} - Frequency ratio without Coriolis effects
FR_C - Frequency ratio including Coriolis effects

TABLE VI. - EFFECT OF CORIOLIS TERMS ON THE STABILITY BOUNDARY FOR PRETWISTED, PRECONED, ROTATING BLADE, MOUNTED OFF THE AXIS OF ROTATION

$a/b = 0.25$, $L/d = 20$, $\varphi = 0$, $\gamma = 45^\circ$

$\frac{\Omega}{\lambda_1}$	$\bar{R}$						
	$\beta_{Pc} = 0^\circ$	$\beta_{Pc} = 15^\circ$		$\beta_{Pc} = 45^\circ$		$\beta_{Pc} = 60^\circ$	
	(a)	(a)	(b)	(a)	(b)	(a)	(b)
2.2	2.385	2.464	2.457	3.406	3.394	5.439	5.414
2.6	1.919	1.962	1.958	2.471	2.462	3.566	3.548
3.0	1.627	1.648	1.645	1.890	1.877	2.390	2.377
4.0	1.241	1.238	1.230	1.107	1.103	.841	.827
5.0	1.060	1.038	1.037	.746	.743	.111	.107
8.0	.859	.823	.823	.348	.347	-----	-----
12.0	.764	.728	.728	.196	.195	-----	-----
16.0	.560	.543	.543	.130	.130	-----	-----
20.0	.411	.386	.386	.041	.041	-----	-----
24.0	.320	.289	.289	-----	-----	-----	-----
40.0	.168	.127	.127	-----	-----	-----	-----
100.0	.060	.014	-----	-----	-----	-----	-----

[a]Coriolis effects disregarded.

[b]Coriolis effects included.

TABLE VII. – EFFECT OF PRETWIST ON THE STABILITY BOUNDARY FOR PRECONED ROTATING BLADE MOUNTED OFF THE AXIS OF ROTATION

$d/b = 0.25$, $\varphi = 0^\circ$ (Coriolis effects included)

γ, degree	Value of $\bar{R}$ for $\beta_{PC} = 15^\circ$ and		Value of $\bar{R}$ for $\beta_{PC} = 45^\circ$ and	
	$\frac{\Omega}{\lambda_1} = 3$	$\frac{\Omega}{\lambda_1} = 20$	$\frac{\Omega}{\lambda_1} = 3$	$\frac{\Omega}{\lambda_1} = 16$
0	1.650	0.407	1.871	0.145
15	1.649	.405	1.872	.143
30	1.647	.398	1.874	.139
45	1.645	.386	1.877	.130
60	1.641	.373	1.882	.115
75	1.636	.358	1.888	.093
90	1.631	.341	1.896	.063

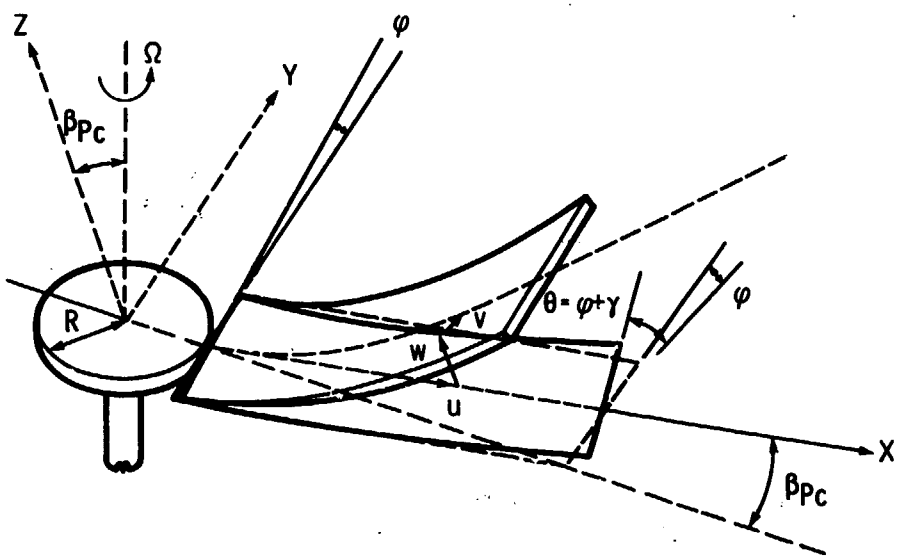

Figure 1. - Blade coordinate system and definition of blade parameters.

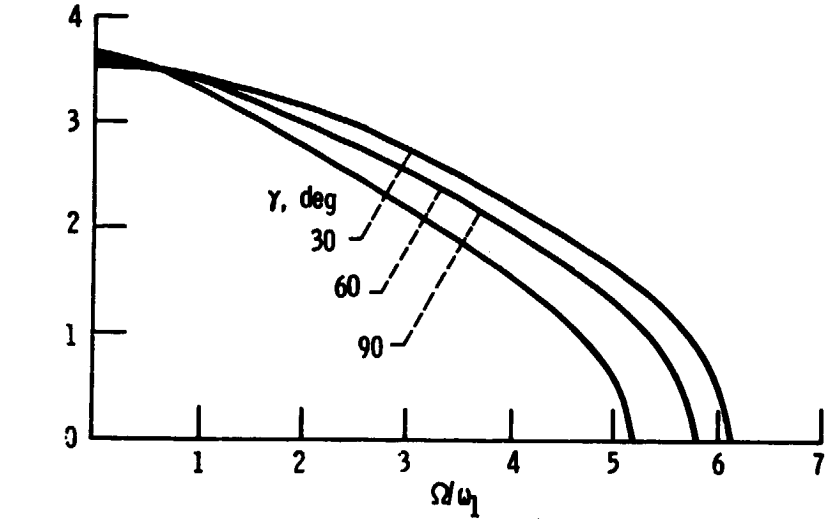

(a) d/b = 0.25, $\beta_{Pc} = 45^0$.

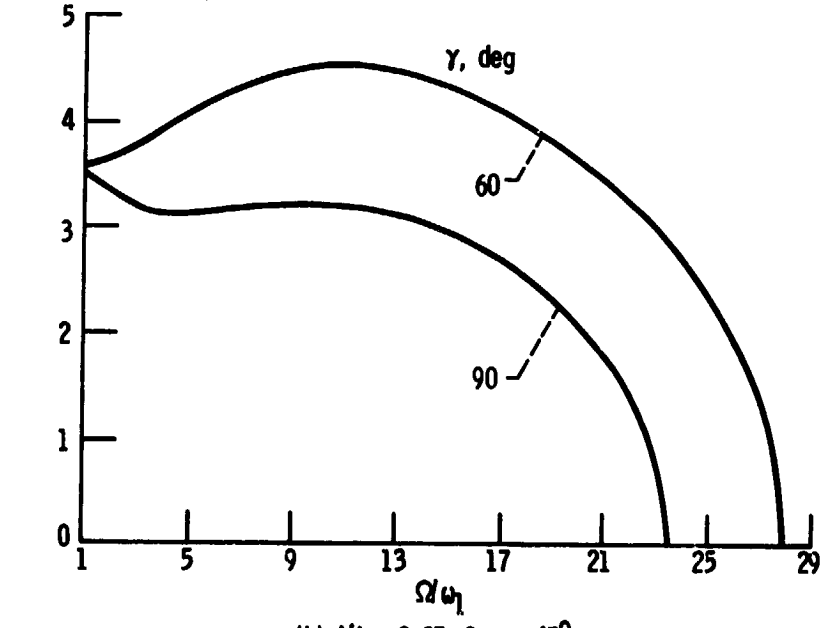

(b) d/b = 0.05, $\beta_{Pc} = 45^0$.

Figure 2. - Effect of variation of pretwist upon the frequency parameter ratio of 45^0 preconed blades at various rotational speeds. (Coriolis effects included)

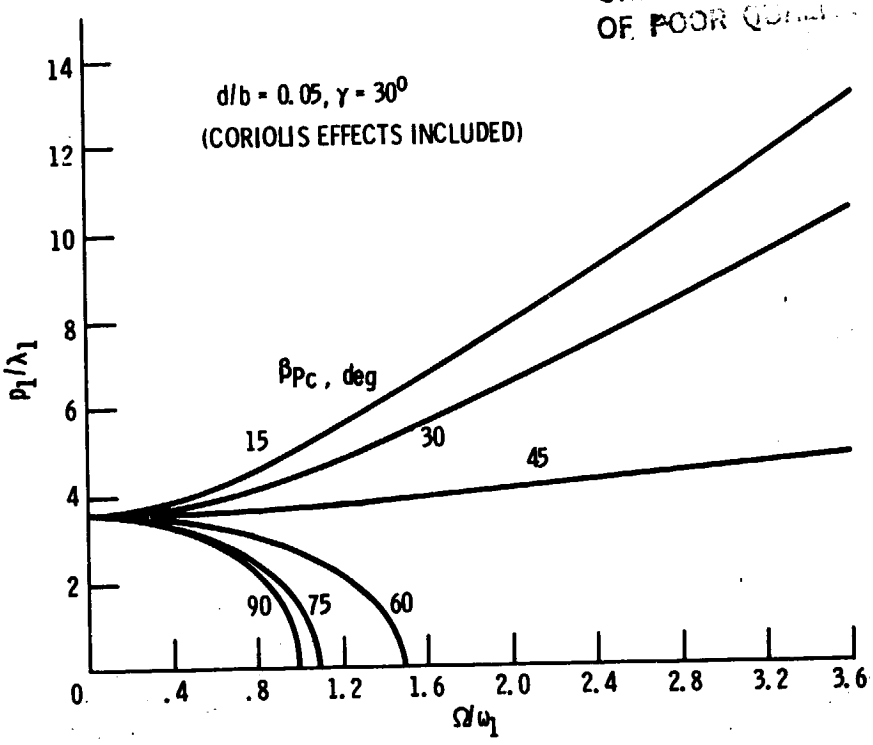

Figure 3. - Effect of variation of precone angle upon the frequency parameter ratios at various rotational speeds of a small thickness ratio pretwisted blade.

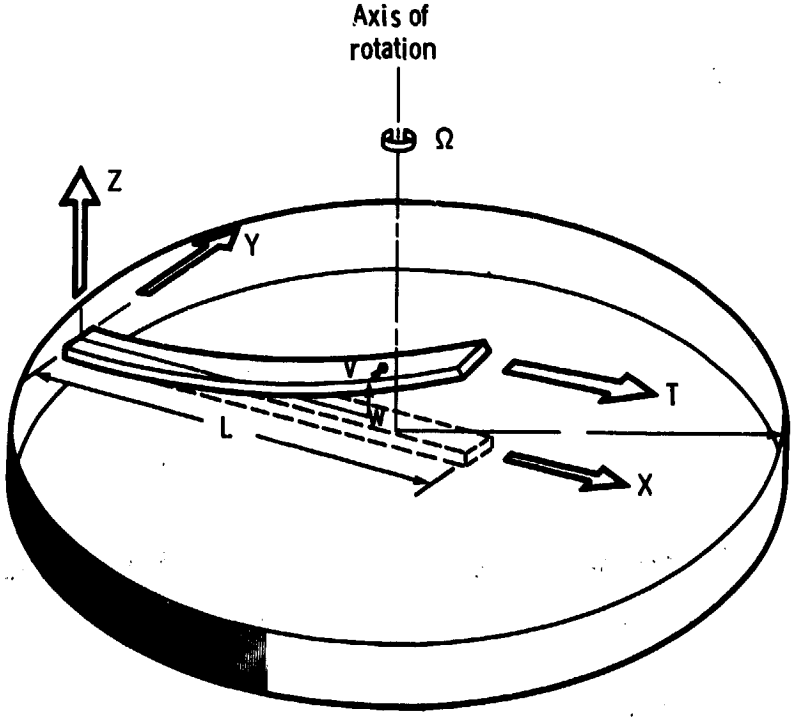

Figure 4. - Rotating beam clamped off the axis of rotation. $\beta_{Pc} = \varphi = \gamma = 0^0$.

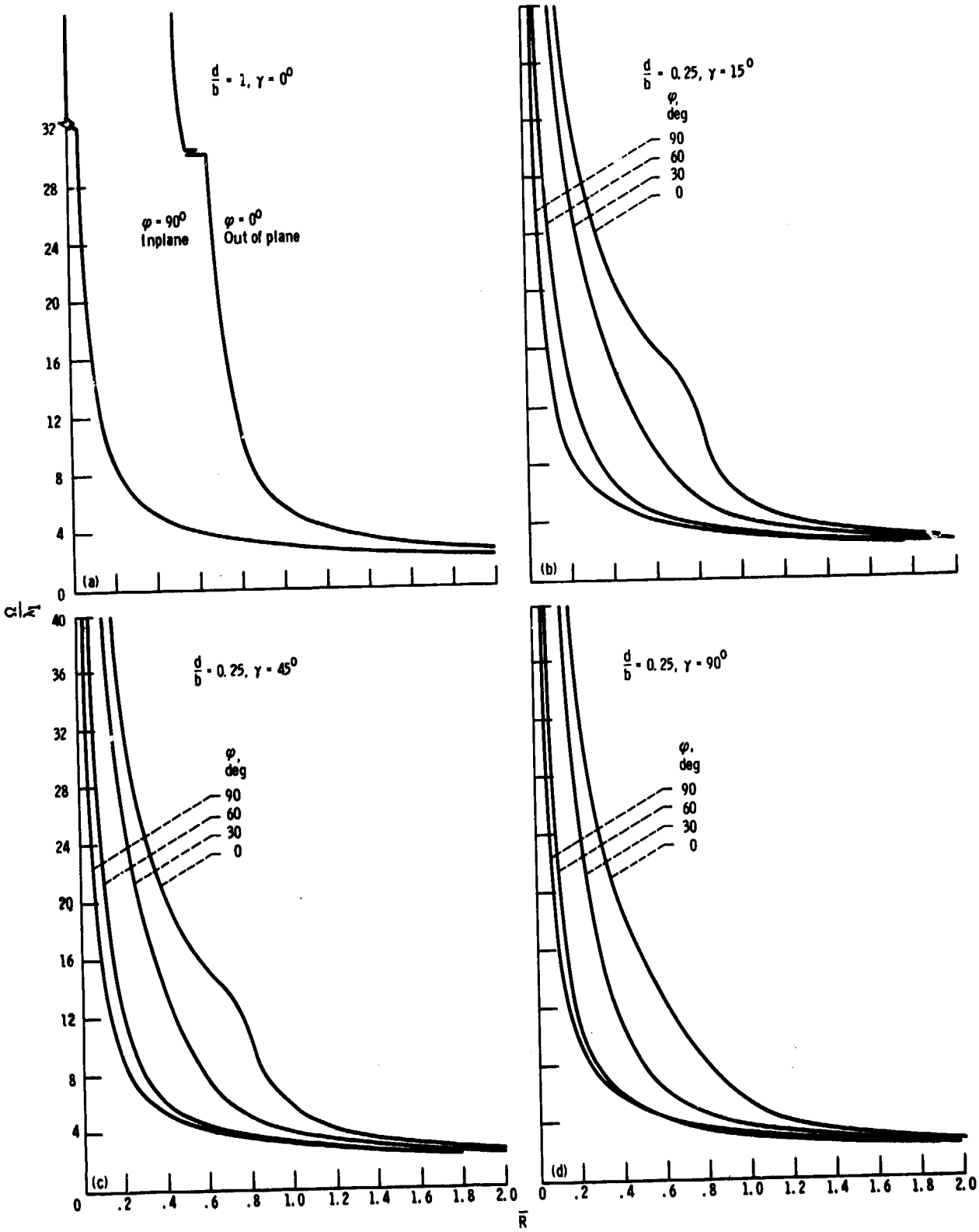

Figure 5. - Critical speed for buckling of rotating pretwisted beams clamped off the axis of rotation: high thickness ratio blade cases.

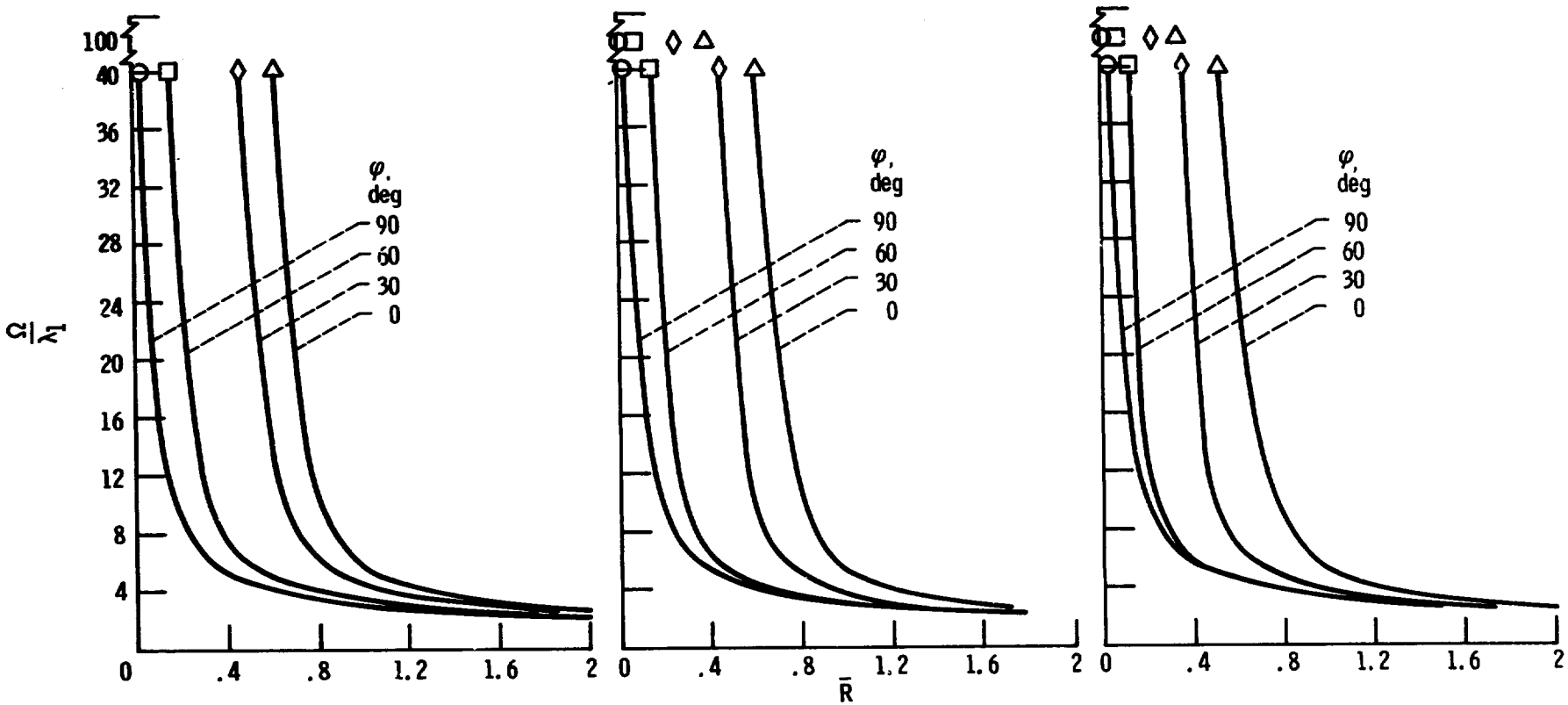

(a) $\frac{d}{b} = 0.05$, $\gamma = 0^{\circ}$.

(b) $\frac{d}{b} = 0.05$, $\gamma = 45^{\circ}$.

(c) $\frac{d}{b} = 0.05$, $\gamma = 90^{\circ}$.

Figure 6. - Critical speed for buckling of rotating pretwisted beams clamped off the axis of rotation: low thickness ratio blade cases.

1. Report No.	2. Government Accession No.	3. Recipient's Catalog No.
NASA TM-87004		

4. Title and Subtitle	5. Report Date
Vibration and Buckling of Rotating, Pretwisted, Preconed Beams Including Coriolis Effects	6. Performing Organization Code 505-33-42

7. Author(s)	8. Performing Organization Report No.
K.B. Subrahmanyam and K.R.V. Kaza	E-2310
	10. Work Unit No.

9. Performing Organization Name and Address	11. Contract or Grant No.
National Aeronautics and Space Administration Lewis Research Center Cleveland, Ohio 44135	13. Type of Report and Period Covered Technical Memorandum

12. Sponsoring Agency Name and Address	14. Sponsoring Agency Code
National Aeronautics and Space Administration Washington, D.C. 20546	

15. Supplementary Notes

K.B. Subrahmanyam, on leave from N.B.K.R. Institute of Science & Technology, Vidyanagar-524 413, India; presently NRC-NASA Research Associate; K.R.V. Kaza, Lewis Research Center. Report prepared for the 10th Biennial Design Engineering Conference and Exhibit on Mechanical Vibration and Noise, sponsored by the American Society of Mechanical Engineers, Cincinnati, Ohio, September 10-13, 1985.

16. Abstract

The effects of pretwist, precone, setting angle and Coriolis forces on the vibration and buckling behavior of rotating, torsionally rigid, cantilevered beams are studied in this investigation. The beam is considered to be clamped on the axis of rotation in one case, and off the axis of rotation in the other. Two methods are employed for the solution of the vibration problem: one based upon a finite-difference approach using second order central differences for solution of the equations of motion, and the other based upon the minimum of the total potential energy functional with a Ritz type of solution procedure making use of complex forms of shape functions for the dependent variables. Numerical results obtained by using these methods are compared to those existing in the literature for specialized simple cases. Results indicating the individual and collective effects of pretwist, precone, setting angle, thickness ratio and Coriolis forces on the natural frequencies and the buckling boundaries are presented and discussed. Furthermore, it is shown that the inclusion of Coriolis effects is necessary for blades of moderate to large thickness ratios while these effects are not so important for small thickness ratio blades. Finally, the results show the possibility of buckling due to centrifugal softening terms for large values of precone and rotation.

17. Key Words (Suggested by Author(s))	18. Distribution Statement
Blades; Vibration; Finite-difference method; Ritz method; Rotation; Pretwist; Precone; Coriolis effects; Buckling	Unclassified - unlimited STAR Category 39

19. Security Classif. (of this report)	20. Security Classif. (of this page)	21. No. of pages	22. Price*
Unclassified	Unclassified		

*For sale by the National Technical Information Service, Springfield, Virginia 22161